

How are physiological responses to drought modulated by water relations and leaf economics' traits in woody plants?

Luca Da Sois^{a,b,*}, Maurizio Mencuccini^{a,c,2}, Eva Castells^{a,b,3}, Pablo Sanchez-Martinez^{a,b,4}, Jordi Martínez-Vilalta^{a,b,c,5}

^a CREAF, Cerdanyola del Vallès, Catalonia 08193, Spain

^b Universitat Autònoma de Barcelona, Cerdanyola del Vallès, Catalonia 08193, Spain

^c ICREA, Barcelona, Spain

ARTICLE INFO

Handling Editor J.E. Fernández

Keywords:

Leaf turgor loss point
Drought stress
Trait coordination
Physiological responses
Leaf economic spectrum
Water relations

ABSTRACT

Species' drought resistance is determined by a combination of multiple traits and their plastic response. However, a clear understanding of how these traits are coordinated and modulate plant responses to drought is still lacking.

Here we used a water exclusion experiment on 20 Mediterranean woody species to evaluate a new framework to study plant drought responses, in which relatively constant functional traits modulate the physiological responses to a given drought exposure. In particular, we assessed how the response of stomatal conductance (G_s), leaf relative water content (RWC) and leaf water potential difference ($\Delta\psi$) to leaf predawn water potential (Ψ_{pd}) were modulated by commonly used functional traits. The latter included hydraulic and water relations attributes such as turgor loss point in leaves (Ψ_{tlp}), vulnerability to xylem embolism in stems (Ψ_{50}), hydraulic conductivity per unit sapwood (K_s), hydraulic conductivity per unit leaf area (K_l , hydraulic sufficiency) and Huber value (H_v), as well as specific leaf area (SLA) as a proxy for the leaf economics spectrum.

Our results show that functional traits are highly coordinated, defining two main axes: the first related to drought tolerance and resource-use strategies and the second characterising the hydraulic sufficiency of leaves. These two axes, as well as many of the underlying functional traits, showed a significant interaction with Ψ_{pd} in explaining physiological responses to drought, thus modulating G_s , RWC, and $\Delta\psi$ responses. Drought-tolerant species showed a less stringent regulation of water use and leaf water potential but were more effective at regulating leaf RWC. Also, the leaf water potential at turgor loss (Ψ_{tlp}) emerged as an important trait orchestrating plant responses to drought.

This study highlights that a clear separation between slow-varying traits (Ψ_{tlp} , Ψ_{50} , K_s , K_l , H_v , SLA), physiological responses (G_s , RWC, $\Delta\psi$) and tissue-level exposure to drought (Ψ_{pd}) improves our understanding of plant drought resistance strategies.

1. Introduction

Forest ecosystems are severely impacted by changes in temperature and precipitation regimes driven by global change, leading to longer and more intense extreme climatic events (McDowell et al., 2020; Seidl et al., 2017). Drought is the most widespread stress factor altering forest

functioning and carbon balance, potentially leading to extensive forest dieback events (Allen et al., 2015; Brodribb et al., 2020). Therefore, it is of paramount importance to improve our capacity to predict how forests will respond to global change-type droughts and what species and forest types are more vulnerable (Anderegg et al., 2022; Lecina-Díaz et al., 2021).

* Corresponding author at: CREAF, Cerdanyola del Vallès, Catalonia 08193, Spain.

E-mail address: l.dasois@creaf.uab.cat (L. Da Sois).

¹ <https://orcid.org/0000-0002-1170-7410>

² <https://orcid.org/0000-0003-0840-1477>

³ <https://orcid.org/0000-0001-7423-2742>

⁴ <https://orcid.org/0000-0002-0157-7800>

⁵ <https://orcid.org/0000-0002-2332-7298>

Drought-induced mortality is usually triggered by the loss of water transport capacity in the plant xylem, known as hydraulic failure (Choat et al., 2018). Under drought conditions, generally accompanied by high temperatures and high evaporative demand, xylem tensions increase, increasing the risk of air bubbles expanding inside the conduits and ultimately blocking water flow. Stomata tend to close before substantial hydraulic losses are observed in the xylem, thus reducing water loss and limiting xylem tensions (Bartlett et al., 2016). Even after stomatal closure, xylem tension continues to increase slowly, as some water is lost due to cuticle conductance and stomatal leakage (Duursma et al., 2019). If drought continues, xylem tension reaches a critical threshold where emboli start to spread through the xylem, causing a hydraulic dysfunction that, under persistent drought conditions, can lead to a systemic vascular failure resulting in tissue drying out and ultimately causing plant death (McDowell et al., 2022).

It has been hypothesised that leaf-level resource-use strategies are related to hydraulic strategies, defining a single plant economics spectrum, running from acquisitive (i.e., “fast-growing”) plants with high rates of resource acquisition and use at the organ and individual scales to conservative (i.e., “slow-growing”) plants with opposite characteristics (Reich, 2014). Thus, more acquisitive plants would show a faster growth rate and rely on a more efficient water transport with higher hydraulic conductivity (Liu et al., 2021 but see Gleason et al., 2016), with lower-density xylem and less-durable leaves. There is some evidence that “fast-growing” plants are more vulnerable to xylem embolism (Oliveira et al., 2021) and hence less able to tolerate low water potentials in their tissues. To resist drought, these “fast-growing” plants would tend to display the so-called “drought avoidance strategy” relying on stringent stomatal control and leaf shedding to reduce water loss during intense drought events. “Slow-growing” plants, instead, would rely on the safety of their water transport system and their lower leaf turgor loss point.

Despite this emergent knowledge, many aspects of trait coordination and how it corresponds to drought resistance strategies are far from being totally understood (Kannenberg et al., 2022; Rosas et al., 2021). Here, we define drought resistance as the ability to function and survive under low water availability, whereas drought tolerance is defined as a particular mechanism to achieve resistance to drought, involving the ability to endure low water potentials in plant tissues (Levitt, 1980). It has been shown, for instance, that at the global scale drought-tolerant species with higher resistance to embolism are able to function at higher water tensions and have a relatively lax (less conservative) control of water losses under drought, suggesting that one single acquisitive vs. conservative axis is not enough to capture the complexities of drought resistance strategies (Flo et al., 2021).

Plant responses to drought involve a hierarchy of interacting factors, and deciphering how this coordination occurs remains one of the main challenges in predicting drought impacts. Here, we propose a novel, simple framework to organise those factors, including exposure to drought, physiological responses over time and underlying functional traits (Kannenberg et al., 2022). The central tenet of the proposed framework is that relatively constant traits (particularly hydraulic traits) modulate the physiological responses to a given drought exposure. By exposure, we mean the level of stress effectively experienced by plant tissues, which is partially controlled by plant attributes. We use the leaf predawn water potential (Ψ_{pd}) as a measure of the intensity of (internal) drought exposure. Time-varying physiological responses include the regulation of water flows, assessed using leaf stomatal conductance (G_s), and the regulation of water status. The latter is characterised using two proxies: the relative water content (RWC) and the difference between midday and predawn water potentials in leaves (i.e., the water potential difference within the plant assuming Ψ_{pd} is a measure of the water potential of the soil explored by the plant, $\Delta\Psi = \Psi_{md} - \Psi_{pd}$). Finally, the underlying traits involve mainly hydraulic and water relations properties, such as the turgor loss point in leaves (Ψ_{tlp}), the vulnerability to xylem embolism in stems (quantified here as the water potential

inducing 50 % loss of xylem conductivity, Ψ_{50}), the transport efficiency of the xylem (sapwood-specific hydraulic conductivity, K_s), the hydraulic sufficiency of the xylem (leaf-specific hydraulic conductivity, K_l ; which corresponds to the overall hydraulic conductivity of the stem divided by the area of leaves being supplied), and the sapwood-to-leaf area ratio (Huber value, H_v) as a measure of the cross-sectional sapwood area supplying water per unit of leaf area demanding water. In addition, we include the specific leaf area (SLA) as an additional trait characterising leaf-level resource-use strategies, as this variable is considered a key indicator of the leaf economics spectrum (Wright et al., 2004).

Here we assessed how physiological responses to drought exposure are modulated by a set of functional traits describing hydraulic and water relations attributes as well as the leaf economic spectrum (Fig. 1). We studied this using a water exclusion experiment on 20 Mediterranean woody plant species spanning a wide range of drought resistance strategies. In particular, we addressed the following questions:

- (1) How are functional traits coordinated in regulating plant responses to contrasting levels of water availability?
- (2) Do the selected functional traits modulate plant responses to drought, and how?
- (3) Which traits are key in modulating plant physiological responses to drought?

Overall, we expect a tight coordination among functional traits and a modulation role of these traits on the water status and water use under drought. We hypothesise that drought tolerant species (i.e., displaying traits related to higher resistance to embolism such as more negative Ψ_{50} and more negative leaf turgor loss point) will experience a less stringent regulation of both water losses and water status under increasing drought compared to species susceptible to drought.

2. Materials and methods

2.1. Study species and experimental design

We selected 20 woody plant species present in the Mediterranean basin spanning a wide range of water use and drought resistance strategies, and representing different growth forms (trees and shrubs) and leaf habits (deciduous and evergreen) (Table 1).

Saplings 2–3 years old and homogeneous in size within species (Table 1) were bought from a tree nursery (Vivers Carex, Cornellà del Terri, Spain) to ensure that the initial growing conditions were similar among all plants. Overall, we choose 24 individuals plus three backup plants per species, for a total of 540 saplings.

The experiment was conducted at the experimental fields of IRTA at Torre Marimon (Caldes de Montbui; 41.613 N, 2.170 E, 176 m a.s.l.), located approximately 30 km north of Barcelona (Catalonia, Spain). The climate is characterised by hot and dry summers and mild winters (Mediterranean climate): the average annual temperature is 14.5 °C and the average annual precipitation is 633 mm.

In December 2018, individual saplings were transplanted into circular-shaped 40 dm³ pots (ø 32 cm at the base, ø 43 cm at the top, height of 37 cm) and randomly placed in a ca. 1000 m² experimental field at a constant distance of 125 cm from one another along eight different lines organised in staggered rows to avoid neighbouring taller plants shading smaller ones. Every pot was filled with a 10 dm³ layer of gravel to ensure drainage at the bottom, followed by an upper 30 dm³ layer of soil at the top. The soil was made of 23 % sand and 77 % mixture of two commercial substrates for plants: J-2 substrate (Burés) containing compost, Sphagnum peat and perlite; and BVU substrate (Burés, Girona, Spain) containing fertiliser NPK 15-7-15, Sphagnum peat and ground pine bark. Also, pots were kept about 5 cm above the ground by placing them on top of upside-down plastic saucers to drain the excess water and avoid direct contact with the soil. The pot soil surface was covered with

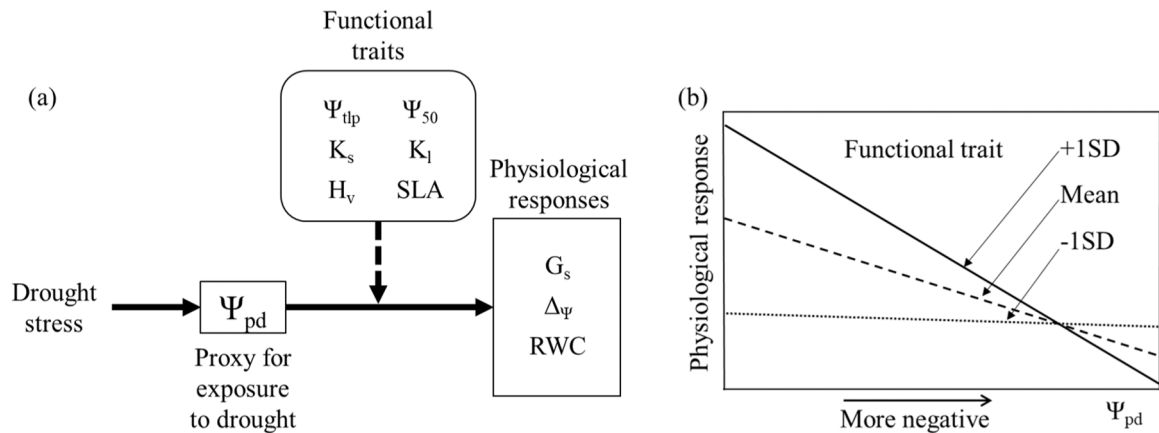


Fig. 1. (a) Summary of the conceptual framework used in this research: drought stress influences the leaf water potential at predawn (Ψ_{pd}), a measure of tissue-level exposure that drives physiological responses. Functional traits are expected to modulate the relationship between Ψ_{pd} and the physiological responses. (b) Example figure for interpreting the modulation effect as reported in the statistical models: in this example, the explanatory trait (i.e., functional trait) significantly modulates the relationship between Ψ_{pd} and the response variable (i.e., physiological response): a higher value of the explanatory trait (mean +1 standard deviation, SD) results in higher sensitivity (steeper relationship) of the response variable to Ψ_{pd} . As a result, a higher value of the explanatory trait results in higher values of the response variable at less negative leaf water potentials, while it results in lower values of the response variable at more negative leaf water potentials after passing a threshold.

Table 1
Plant species used in the water exclusion experiment. We show their abbreviated name (Abbr.), Family; Growth habit: tree (t), shrub (s); Leaf habit: deciduous (d), evergreen (e); Drought resistance group: susceptible (S), intermediate (I), resistant (R); Mean height by species at the beginning of the experiment; and Xylem water potential at which the xylem loses 50 % of its conductivity (Ψ_{50}); Lowest mean annual precipitation (5 %) of the distribution of the species in Catalonia (Villanueva, 2005); Resistance to drought from Niinemets and Valladares (2006). Data for Ψ_{50} come from Sanchez-Martinez et al. (2020) except when indicated otherwise. When data for our species were not available neither in the HydraTRY dataset nor in the literature, the Ψ_{50} values for the closest species from the same genus were used.

| Species | Abbr. | Family | Growth habit | Leaf habit | Drought resistance group | Initial height (cm) | Ψ_{50} (-MPa) | 5 % MAP (mm) | Drought resistance (unitless) |
|------------------------------|-------|---------------|--------------|------------|--------------------------|---------------------|--------------------|------------------|-------------------------------|
| <i>Acer campestre</i> | AC | Aceraceae | t | d | I | 130.0 | 3.02 | 736 | 2.93 |
| <i>Acer monspessulanum</i> | AM | Aceraceae | t | d | R | 62.4 | 3.87 | 530 | 4.31 |
| <i>Alnus glutinosa</i> | AG | Betulaceae | t | d | S | 168.3 | 1.78 | 692 | 2.22 |
| <i>Arbutus unedo</i> | AU | Ericaceae | s | e | R | 94.8 | 5.47 | 501 | 3.9 |
| <i>Betula pubescens</i> | BP | Betulaceae | t | d | S | 181.1 | 2.31 ¹ | 786 ³ | 1.85 |
| <i>Buxus sempervirens</i> | BS | Buxaceae | s | e | R | 45.3 | 8.00 | 623 | 3.88 |
| <i>Crataegus monogyna</i> | CM | Rosaceae | s | d | I | 65.7 | 6.83 | 642 | 3.46 |
| <i>Fraxinus angustifolia</i> | FA | Oleaceae | t | d | S | 188.6 | 3.50 ² | 651 | 2.5 |
| <i>Myrtus communis</i> | MC | Myrtaceae | s | e | I | 53.5 | 6.15 | 396 | |
| <i>Phillyrea latifolia</i> | FL | Oleaceae | s | e | I | 73.0 | 6.78 | 605 | |
| <i>Pinus halepensis</i> | PH | Pinaceae | t | e | R | 111.3 | 4.65 | 431 | 4.97 |
| <i>Pinus sylvestris</i> | PS | Pinaceae | t | e | I | 48.8 | 3.19 | 693 | 4.34 |
| <i>Pistacia lentiscus</i> | PL | Anacardiaceae | s | e | R | 51.3 | 4.76 | 424 | |
| <i>Populus alba</i> | PA | Salicaceae | t | d | S | 163.2 | 1.78 | 395 | 2.67 |
| <i>Quercus coccifera</i> | QC | Fagaceae | s | e | R | 50.4 | 6.94 | 434 | |
| <i>Quercus ilex</i> | QI | Fagaceae | t | e | R | 99.8 | 3.20 | 582 | 4.72 |
| <i>Quercus petraea</i> | QP | Fagaceae | t | d | I | 105.1 | 3.15 | 697 | 3.02 |
| <i>Salix cinerea</i> | SC | Salicaceae | s | d | S | 70.0 | 1.99 | 704 | 0.11 |
| <i>Sambucus nigra</i> | SN | Adoxaceae | s | d | S | 61.1 | 1.36 | 694 | 3.04 |
| <i>Viburnum tinus</i> | VT | Adoxaceae | s | e | I | 50.3 | 1.30 | 363 | |

¹ From Cochard et al. (2005): Ψ_{50} of *Betula pendula*.
² From Cochard et al. (1997): Ψ_{50} of *Fraxinus excelsior*.
³ From Niinemets and Valladares (2006): 5 % MAP of *Betula pendula*.

a coconut palm fibre mulch protection disc to protect the soil from direct sunlight radiation, thus minimising herbal growth and reducing warming and evaporation. All plants were individually watered to field capacity by an automatic dripping system until the onset of the experimental treatments. Plants were exposed to the local environmental conditions, including precipitation.

Twelve randomly selected plants per species (Control group = C) were kept irrigated throughout the whole duration of the experiment, whereas 12 other plants per species (Treatment group = T) were subjected to two sequential drought treatments (Figs. 1S, 2S) after the growing season, once all new leaves had completely developed. The first drought treatment started in early July and the second drought treatment started in early August 2019.

Three groups of species were defined a priori based on each species' expected resistance to drought according to a variety of sources, including the index proposed by Niinemets and Valladares (2006), the current distribution limit of the species in Spain (annual rainfall at the dry limit) and our previous knowledge of the species (García-Valdés et al., 2021; Martínez-Vilalta et al., 2010; Martínez-Vilalta and García-Forner, 2017; Ogaya et al., 2003; Vilà-Cabrera et al., 2015) (Table 1). We also adjusted the grouping to account for the initial size of the individual plants used, which determined that *Phillyrea latifolia* (relatively large plants) was reassigned from Resistant to Intermediate, and *Acer monspessulanum* (relatively small plants) from Intermediate to Resistant. These groups were only employed for experimental purposes, and they were associated with different durations of the drought cycles

(Figs. 1S, 2S): 3 days for the Susceptible group (6 species), 14 days for the Intermediate group (7 species) and 21 for the Resistant group (7 species). By doing so, we expected a relatively constant intensity of drought (relative to their drought resistance) across species. This was also done for practical reasons such that the measurements workload was split among different days allowing measuring an adequate number of replicates per species. The time series of all relevant response variables is provided in the [Supporting Information](#) (Fig. 3S, 8S).

To characterise the species drought resistance and resource-use strategies, measurements were taken before the first drought treatment (mid-June), at the peak of the first drought treatment (July), after a pre-established recovery period of three weeks (end of July – mid-August) and at the peak of the second drought treatment (August–early September). These four campaigns were intended to generate a wide range of water stress conditions similar to the ones experienced by the plants in natural conditions. Additional destructive characterisation measurements were taken at the end of the experiment as described in the next section.

2.2. Species characterisation (trait measurements)

In mid-June 2019, before the first drought treatment, we collected leaf samples (i.e., from one to 30 leaves per individual depending on leaf size to ensure sufficient plant material for measurements) to estimate the leaf water potential at turgor loss point (Ψ_{tlp}) and the specific leaf area (SLA) (Fig. 1S). For Ψ_{tlp} measurements, we sampled leaves from six individuals per species selecting fully expanded, sun-exposed and non-damaged leaves from the upper part of the canopy. Leaves were placed in falcon tubes filled with water for one night in a refrigerator at 4 °C for rehydration. Leaf material was then stored at –80 °C to ensure the breakage of the cell membranes. Measurements were performed in June 2021 using a VAPRO 5520 osmometer (WESCOR, INC, Logan, Utah, USA) on thawed disks of 7 mm in diameter previously punctured with a needle to facilitate evaporation through the cuticle. We measured Ψ_0 (the osmotic potential in hydrated leaves) and calculated the Ψ_{tlp} using the equation proposed by Bartlett et al. (2012a): $\Psi_{tlp} = 0.832 * \Psi_0 - 0.631$. To determine SLA, we sampled leaves from five individuals per species, selecting the second youngest fully expanded, non-damaged and non-shaded leaves from the apex of the branches. Depending on the size of the leaves, a different amount of material per individual was collected for each species (ranging from one compound leaf for *Sambucus nigra* to 30 needles for pine species). Leaves were scanned on the same day of the sampling and the total area (A_{leaves}) was calculated using ImageJ (Huang et al., 2007). Leaves were subsequently dried in an oven at 70 °C for 48 h and weighed to obtain the dry weight (DW_{leaves}). SLA was calculated as the ratio of A_{leaves} to DW_{leaves} .

Additional destructive measurements were performed between late April and early July 2021, after the end of the experiment, to characterise species' hydraulic properties (Fig. 1S). For K_s and K_l , we sampled six individuals per species of which three plants belonged to the control group and three plants belonged to the treatment group, selecting the individuals in the best shape after the experimental campaigns. In doing so we assumed that ontogenetic changes in K_s and K_l during the ~2 years treatment period were relatively small and thus the differences observed among species at the end of the treatment were representative of the situation during the treatment. For *Buxus sempervirens*, we sampled four individuals only due to a lack of plant material in good conditions. Branches of approx. 80 cm were cut at noon, stored in a fridge at 4 °C in the dark, and measured within 24 h from the time of sampling.

Measurements of hydraulic conductivity were performed following Rosas et al. (2019) using a commercial XYL'em apparatus (Bronkhorst, Montigny-Les-Cormeilles, France). Before starting the measurements, the branches were progressively re-cut under water with hand pruners to favour the relaxation of the xylem pressures to avoid cutting artefacts (Wheeler et al., 2013). The final segment was 2–5 cm long depending on the species and was always selected at the same distance from the apex

within a given species. The cut ends were trimmed three times with a razor blade to get a clean surface, debarked at both ends (Savi et al., 2019) and carefully connected to the tubing system of the XYL'em apparatus paying attention that no air bubbles were present within the tubing system.

Samples were perfused with a degassed (Liqui-Cell membrane contactor MM-1.7 × 5.5 Series; Charlotte, NC, USA) deionised and filtered perfusion solution enriched with 10 mM KCl and 1 mM $CaCl_2$ (Rosas et al., 2019) and were flushed at 180 kPa for 20 min (for Angiosperm species) or kept in the same solution under a partial vacuum for 48 h (for Gymnosperm species) (Rosas et al., 2019). The maximum conductivity (K_{max}) was then measured as the water flow through the xylem at an applied pressure gradient of 5 kPa. The measurement was recorded 2 min after the start of the water flow when readings stabilised. Both the XYL'em apparatus and its tubing system were cleaned weekly using a solution of 10 % bleach for 30 min to prevent micro-organisms growth and were also flushed twice with the perfusion solution to remove any trace of bleach and impurity from the system before actual measurements were taken.

All leaves present in the distal part of the segment were collected and dried in an oven at 70 °C for two days and weighed to obtain their dry weight (DW_{leaves}). The overall leaf area was obtained as the product between SLA and DW_{leaves} , making use of the previously measured SLA at the species level. The stem-specific hydraulic conductivity (K_s) was calculated as K_{max} divided by the cross-sectional sapwood area (removing the area occupied by the pith and the bark), and the leaf-specific hydraulic conductivity (K_l) was calculated as K_{max} divided by the distal leaf area. The Huber value (H_v) was calculated as the xylem cross-sectional area (i.e., without bark and pith) over the distal leaf area (A_{leaves}). To estimate the vulnerability to embolism for all species we used the Ψ_{50} obtained from the HydrATRY database (Sanchez-Martinez et al., 2020) and additional literature sources when needed (see Table 1).

2.3. Monitoring drought responses in terms of water status and use

During the four monitoring campaigns (before drought, 1st drought, recovery, 2nd drought) we measured the leaf water potential at predawn (Ψ_{pd}) and midday (Ψ_{md}), the relative water content of the leaves (RWC) and the leaf stomatal conductance to water vapour (G_s) (Fig. 1S). Measurements during all the monitoring campaigns were performed on the same individual trees whenever possible. In the few cases when individual trees needed to be substituted (e.g. due to insect outbreaks), the new individual tree was chosen as being as similar in size as possible.

For Ψ_{pd} and Ψ_{md} , we sampled six individual plants per treatment and species between 3:30 and 4:30 am for the former and between 11:30 am and 12:30 pm for the latter (solar times in all cases). Apical, non-damaged and sun-exposed branches were excised and immediately placed in plastic bags into which air was exhaled to humidify the environment and stored in a fridge. Samples were measured within 4 h from the time of sampling with a Scholander bomb (Model 1000 Pressure Chamber Instrument, PMS Instrument Company, Albany, Oregon, USA; or a Digital pressure chamber SF-Pres-40 Solfranc Tecnologias SL, Tarragona, Spain). We measured terminal twigs in all species except for *Sambucus nigra* in which we performed our measurements on compound leaves. The leaf water potential difference ($\Delta\Psi$) was calculated as $\Psi_{md} - \Psi_{pd}$.

We also measured the leaf RWC using the gravimetric method (Fernández-García et al., 2014): for six individuals per species and treatment (three individuals for the initial campaign) we sampled (between 9:00 and 10:00 am, solar time) the second youngest, fully-grown and not shaded apical leaves (one to 12 depending on the species) and stored them in a fridge in pre-weighted falcon tubes and quickly measured their fresh mass (FW) upon the arrival to the laboratory. Leaves were rehydrated by filling the vials to overflow and stored in the fridge overnight at 4 °C and then carefully bolt-dried with a paper towel

and measured the turgid weight (TW). Leaves were later on placed in an oven at 70° for 24 h until constant weight and their dry weight (DW) were measured. RWC was calculated as:

$$RWC (\%) = 100 \left(\frac{FW - DW}{TW - DW} \right)$$

Finally, for six individuals per species and treatment, we measured G_s on three undamaged, fully-grown and sun-exposed leaves using a Decagon porometer (Decagon Devices SC-1, Pullman, Washington, USA). The mean of the three measurements for each individual plant was recorded. The measurements were performed from 10:00 am to 6:00 pm under sunny conditions and later on standardised to reference conditions of VPD and time of the day to make them fully comparable. This standardisation was achieved by using a random-intercept linear mixed model of G_s as a function of VPD and time of the day (fixed effects) and with species, campaign and treatment as random effects. This model was used to estimate G_s at noon and for VPD = 1 kPa for each species and date.

2.4. Statistical analyses

We performed a principal component analysis (PCA) with the species-averaged values of the selected functional traits (Ψ_{tlp} , Ψ_{50} , K_s , K_l , H_v , SLA) previously log-transformed and scaled in order to characterise the species' water-use and drought response strategies. Prior to making the PCA, we made sure our data met the assumptions of the analysis. Axes were rotated using the 'oblimin' function (available in the "psych" R package) for better interpretation. The eigenvalues of the first two 'oblimin'-rotated components (namely PC₁ and PC₂) were extracted. We also applied a "varimax" rotation (also available in the "psych" R package) and used both two and three PCA axes, obtaining similar results (Table 1S, Fig. 9S).

We used linear mixed models to test the effect of the functional traits (i.e., explanatory traits) on the relationship between the physiological responses related to the regulation of water status and water use (G_s , $\Delta\psi$ or RWC, hereafter response variables) and Ψ_{pd} as a measure of soil water availability and exposure to drought (Fig. 1). We considered treatment and species as crossed random effects in our models:

$$Resp\ var = \Psi_{pd} * Expl\ trait + (1|Treatment) + (1|Species)$$

Data for all explanatory traits (except for PC₁, PC₂) and Ψ_{pd} were log-transformed (after changing the sign to positive when needed) to comply with the assumptions of normality and homoscedasticity and were later on scaled (subtracting the mean and dividing by the standard deviation) for better interpretation of the data. Data analysis was performed using R v.3.6.1 (R Core Team, 2019) using the packages "factoextra", "lme4", "lmerTest" and "interactions". Graphs were performed using the packages "ggplot2", and "ggpubr". PCA rotation was performed using the package "psych".

3. Results

3.1. Traits coordination

The functional traits of the studied species were distributed along two dimensions that together accounted for almost 70 % of the overall trait variability (Fig. 2). The first axis (PC₁) was mostly driven by SLA and K_s on one side and Ψ_{50} and Ψ_{tlp} on the other, and can be interpreted as a proxy for drought tolerance and conservative resource use. The second axis (PC₂) was driven by K_l and to a lower extent H_v and can be understood as a measure of the hydraulic sufficiency of leaves. Our interpretation of the first axis is consistent with the fact that all the species that we originally classified as susceptible to drought are located on the left-hand side of this axis, whereas those designed as drought resistant are located on the right-hand side of PC₁ (more negative Ψ_{tlp}

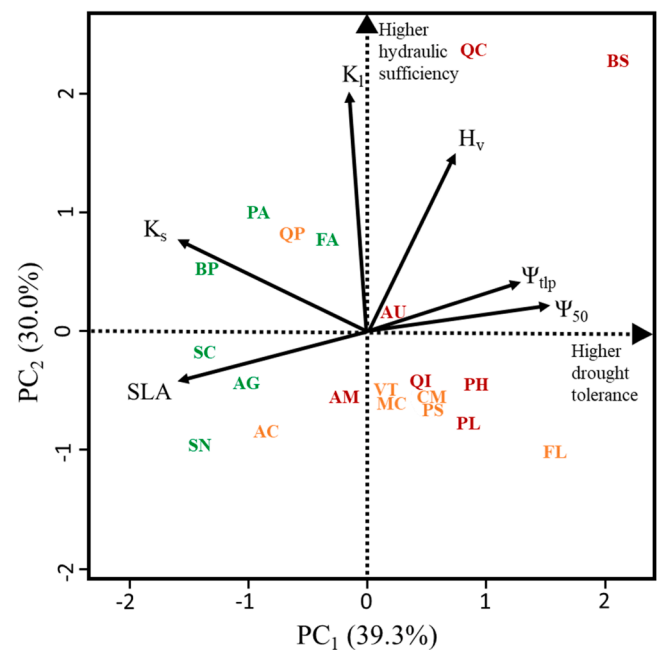


Fig. 2. Biplot showing trait and species distributions in the space obtained by an 'oblimin'-rotated principal component analysis. Our species are distributed along two main axes of variability: PC₁ is driven by leaf structural properties (SLA), xylem water transport capacity (K_s), xylem vulnerability to embolism (Ψ_{50}) and leaf water potential at turgor loss (Ψ_{tlp}), water status regulation properties; PC₂ is driven by traits describing the hydraulic sufficiency of leaves (K_l) and the plant allocation to sapwood relative to leaves (H_v). Colours indicate the drought resistance group of the species: susceptible (green), intermediate (orange), and resistant (red). Our species are highly diverse in terms of water-use strategy. See Table 1 for the full names of the species.

and Ψ_{50}). The first PCA axis also segregated between deciduous species (on the left-hand side) and evergreen species (on the right-hand side). No clear pattern arises from the distribution of our species along PC₂, suggesting that different combinations of strategies of hydraulic sufficiency and allocation are possible irrespectively to the overall drought resistance of the species.

3.2. Trait effects modulating drought responses

In all our models relating physiological responses to the interaction between functional traits and drought exposure the direct effect of exposure (Ψ_{pd}) was highly significant (Table 2), while the direct effects of the explanatory traits were not significant except for the effect of Ψ_{tlp} onto $\Delta\psi$. The interactions between Ψ_{pd} and the studied explanatory traits were significant in 14 out of 24 models (Table 2).

For the models using aggregate, PCA-based metrics to characterize traits (Fig. 2), PC₁ (drought tolerance axis) modulated the relationship between Ψ_{pd} and the three response variables (Fig. 3). Higher values of PC₁ (more negative Ψ_{50} , Ψ_{tlp}) resulted in a steeper relationship between Ψ_{pd} and $\Delta\psi$, with larger $\Delta\psi$ at less negative Ψ_{pd} and smaller $\Delta\psi$ at more negative Ψ_{pd} compared to plants with lower values of PC₁ (high SLA, high K_s). Also, higher values of PC₁ were associated with a shallower relationship between Ψ_{pd} and both G_s and RWC, showing lower values of G_s and RWC at less negative Ψ_{pd} and higher values of G_s and RWC at more negative Ψ_{pd} , compared to plants with lower values of PC₁. PC₂ (leaf hydraulic sufficiency axis) only modulated the relationship between Ψ_{pd} and RWC (Fig. 3): higher values of PC₂ (high hydraulic sufficiency) were associated with a less steep relationship between Ψ_{pd} and RWC, compared to plants with lower values of PC₂ (low H_v , low K_l).

Zooming into individual trait effects modulating the relationships between Ψ_{pd} and the three response variables, the results were highly

Table 2

Estimated coefficients of the generalised linear models relating the response variables (G_s , $\Delta\psi$, RWC) with tissue-level exposure to drought (Ψ_{pd}), functional traits (i.e., explanatory traits) and their interaction. Panel (a) shows PC₁, PC₂ as synthetic explanatory traits, whereas part (b) shows the effect of individual traits (Ψ_{tlp} , Ψ_{50} , K_s , K_l , H_v , SLA). Significant interactions are in bold.

| (a) | | | | Response variables | | | | | | | |
|-------------------------------|----------|------------|------------------|--------------------|------------|------------------|--------------|------------|------------------|-----|--|
| | | | | G_s | | | $\Delta\psi$ | | | RWC | |
| Effect | Estimate | Std. Error | p | Estimate | Std. Error | p | Estimate | Std. Error | p | | |
| (Intercept) | 366.966 | 44.291 | 0.002 | 10.901 | 0.721 | <0.001 | 81.700 | 1.595 | <0.001 | | |
| Ψ_{pd} | -114.568 | 13.264 | <0.001 | -4.363 | 0.288 | <0.001 | -3.870 | 0.401 | <0.001 | | |
| PC ₁ | -50.075 | 34.571 | 0.165 | 0.522 | 0.740 | 0.490 | 0.866 | 1.031 | 0.412 | | |
| Ψ_{pd} : PC ₁ | 49.107 | 14.423 | 0.001 | -1.202 | 0.324 | <0.001 | 1.349 | 0.446 | 0.003 | | |
| (Intercept) | 372.160 | 45.142 | 0.001 | 10.774 | 0.748 | <0.001 | 81.837 | 1.467 | <0.001 | | |
| Ψ_{pd} | -105.370 | 13.181 | <0.001 | -4.596 | 0.287 | <0.001 | -3.405 | 0.398 | <0.001 | | |
| PC ₂ | 11.113 | 36.605 | 0.765 | 0.614 | 0.768 | 0.435 | 0.153 | 1.036 | 0.885 | | |
| Ψ_{pd} : PC ₂ | -2.766 | 14.577 | 0.850 | 0.132 | 0.325 | 0.685 | 1.399 | 0.451 | 0.002 | | |

| (b) | | | | Response variables | | | | | | | |
|----------------------------|----------|------------|------------------|--------------------|------------|------------------|--------------|------------|------------------|-----|--|
| | | | | G_s | | | $\Delta\psi$ | | | RWC | |
| Effect | Estimate | Std. Error | p | Estimate | Std. Error | p | Estimate | Std. Error | p | | |
| (Intercept) | 368.323 | 44.128 | 0.001 | 10.888 | 0.594 | <0.001 | 81.686 | 1.561 | <0.001 | | |
| Ψ_{pd} | -111.128 | 13.334 | <0.001 | -4.450 | 0.287 | <0.001 | -3.860 | 0.403 | <0.001 | | |
| Ψ_{tlp} | -13.920 | 35.025 | 0.696 | 1.892 | 0.595 | 0.005 | 0.968 | 1.007 | 0.349 | | |
| Ψ_{pd} : Ψ_{tlp} | 29.168 | 13.829 | 0.035 | -0.859 | 0.309 | 0.006 | 1.105 | 0.413 | 0.008 | | |
| (Intercept) | 369.473 | 44.658 | 0.001 | 10.813 | 0.720 | <0.001 | 81.755 | 1.588 | <0.001 | | |
| Ψ_{pd} | -109.805 | 13.094 | <0.001 | -4.556 | 0.285 | <0.001 | -3.763 | 0.402 | <0.001 | | |
| Ψ_{50} | -24.020 | 34.803 | 0.499 | 0.854 | 0.719 | 0.250 | 0.948 | 1.002 | 0.356 | | |
| Ψ_{pd} : Ψ_{50} | 32.855 | 12.575 | 0.009 | -0.437 | 0.284 | 0.125 | 0.725 | 0.411 | 0.078 | | |
| (Intercept) | 371.748 | 44.059 | 0.002 | 10.785 | 0.738 | <0.001 | 81.827 | 1.593 | <0.001 | | |
| Ψ_{pd} | -107.958 | 12.973 | <0.001 | -4.505 | 0.280 | <0.001 | -3.640 | 0.395 | <0.001 | | |
| K_s | 66.311 | 33.262 | 0.061 | 0.562 | 0.740 | 0.457 | -0.771 | 1.003 | 0.452 | | |
| Ψ_{pd} : K_s | -32.765 | 11.904 | 0.006 | 1.020 | 0.266 | <0.001 | -0.574 | 0.379 | 0.131 | | |
| (Intercept) | 372.207 | 44.901 | 0.001 | 10.777 | 0.757 | <0.001 | 81.873 | 1.451 | <0.001 | | |
| Ψ_{pd} | -104.825 | 13.249 | <0.001 | -4.595 | 0.289 | <0.001 | -3.371 | 0.399 | <0.001 | | |
| K_l | 10.002 | 35.708 | 0.783 | 0.362 | 0.758 | 0.639 | 0.041 | 1.009 | 0.968 | | |
| Ψ_{pd} : K_l | 0.786 | 14.014 | 0.955 | 0.113 | 0.312 | 0.719 | 1.374 | 0.426 | 0.001 | | |
| (Intercept) | 372.120 | 44.467 | 0.001 | 10.773 | 0.760 | <0.001 | 81.855 | 1.482 | <0.001 | | |
| Ψ_{pd} | -103.561 | 13.146 | <0.001 | -4.707 | 0.285 | <0.001 | -3.350 | 0.400 | <0.001 | | |
| H_v | -18.650 | 35.722 | 0.608 | 0.094 | 0.763 | 0.904 | 0.671 | 0.990 | 0.507 | | |
| Ψ_{pd} : H_v | 11.133 | 14.642 | 0.447 | -0.578 | 0.328 | 0.079 | 1.542 | 0.467 | 0.001 | | |
| (Intercept) | 368.616 | 43.925 | 0.001 | 10.831 | 0.753 | <0.001 | 81.701 | 1.583 | <0.001 | | |
| Ψ_{pd} | -110.853 | 13.383 | <0.001 | -4.514 | 0.291 | <0.001 | -3.824 | 0.399 | <0.001 | | |
| SLA | 37.670 | 34.135 | 0.284 | -0.134 | 0.754 | 0.860 | 0.282 | 1.018 | 0.785 | | |
| Ψ_{pd} : SLA | -29.360 | 14.311 | 0.041 | 0.479 | 0.322 | 0.137 | -1.299 | 0.430 | 0.003 | | |

consistent with those obtained for PCA axes, showing opposite effects for Ψ_{tlp} and Ψ_{50} compared to SLA and K_s (Fig. 4a). For the traits contributing to PC₁: a more negative Ψ_{tlp} resulted in a steeper relationship between Ψ_{pd} and $\Delta\psi$, with higher $\Delta\psi$ regardless of the values of Ψ_{pd} in comparison to plants with less negative Ψ_{tlp} . The differences in $\Delta\psi$ due to the modulation effect of Ψ_{tlp} become minimal at more negative Ψ_{pd} . Conversely, a more negative Ψ_{tlp} , resulted in a flatter relationship between Ψ_{pd} and both G_s and RWC. Ψ_{50} only modulated the relationship between Ψ_{pd} and G_s (Fig. 4a). Similarly to Ψ_{tlp} , a more negative Ψ_{50} resulted in a flatter relationship between Ψ_{pd} and G_s . The interaction between Ψ_{50} and Ψ_{pd} was marginally significant and the effect was in the same direction as that of Ψ_{tlp} . K_s also modulated the relationships between Ψ_{pd} and both $\Delta\psi$ and G_s , but not the relationship between Ψ_{pd} and RWC (Fig. 4b). As expected, the effect of K_s was opposite to that of Ψ_{50} and Ψ_{pd} : higher values resulted in a flatter relationship between Ψ_{pd} and $\Delta\psi$, and in a steeper relationship between Ψ_{pd} and G_s . Finally, SLA modulated the relationships between Ψ_{pd} and both G_s and RWC, but not the relationship between Ψ_{pd} and $\Delta\psi$ (Fig. 4a). A higher SLA resulted in a steeper relationship between Ψ_{pd} and both G_s and RWC, with higher values of G_s and RWC at less negative Ψ_{pd} and similar or lower values of G_s at more negative Ψ_{pd} .

Regarding the individual traits contributing to PC₂ (K_l and H_v), their effects were also consistent with those of the overall axis (Fig. 4b): they only modulated the relationship between Ψ_{pd} and RWC, with higher K_l and H_v , resulting in a flatter relationship between Ψ_{pd} and RWC, with lower values of RWC at less negative Ψ_{pd} and higher values of RWC at

more negative Ψ_{pd} in comparison to plants with a lower K_l and H_v , respectively.

4. Discussion

We found that functional traits are highly coordinated in regulating plant responses to water availability fluctuations, either contributing to defining the overall resource use strategy and drought tolerance of the species (Ψ_{tlp} , Ψ_{50} , K_s , SLA) or determining their hydraulic sufficiency (K_l , H_v). In addition, we applied a new framework linking functional traits with plant physiological responses to drought exposure, the latter characterised using the leaf water potential at predawn (Ψ_{pd}). Our results show that the regulation of water status and use emerges from the interaction between Ψ_{pd} and the studied functional traits and suggests a central role of Ψ_{tlp} in orchestrating physiological responses to drought.

4.1. Functional traits coordination

Our results show that species are distributed along two main axes of variability described by the functional traits studied (Fig. 2). The first axis (PC₁) describes drought tolerance (more negative Ψ_{tlp} and Ψ_{50}) and conservatism in resource use (low K_s and SLA). Those results are in agreement with previous studies assessing drought resistance strategies (Markestijn et al., 2011; Rosas et al., 2021) and reflect to some extent the expectations of a plant economics spectrum (Reich, 2014) describing a continuum from more conservative to more acquisitive strategies, the

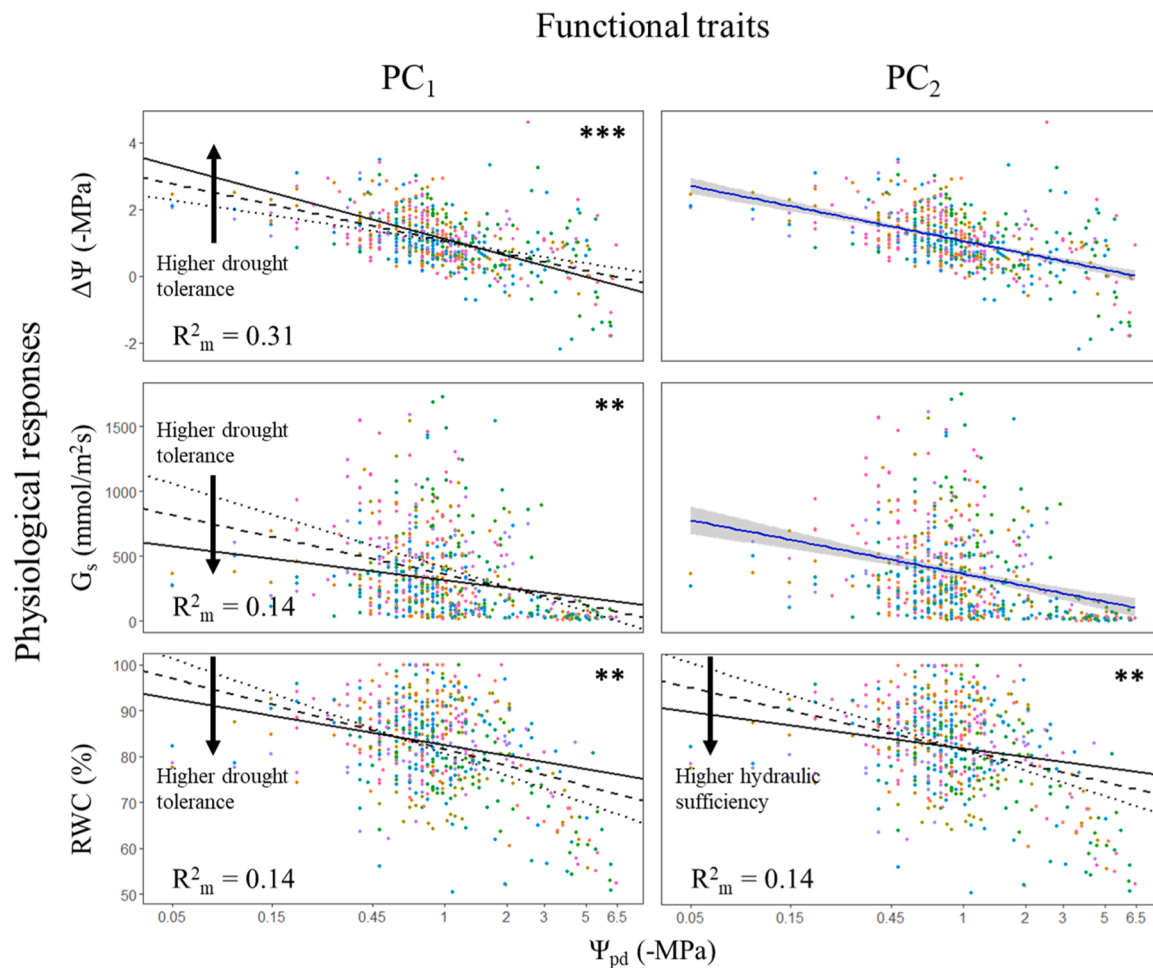


Fig. 3. Interaction plots of the relationship between physiological responses (G_s , $\Delta\Psi$, RWC) and tissue-level exposure to drought (Ψ_{pd}), modulated by functional traits (i.e., explanatory traits), using the first two rotated components (PC₁, PC₂) as integrative measures of the latter. The black continuous line represents the relationship between Ψ_{pd} and the response variable for values corresponding to the mean plus one standard deviation (+1 SD) of the trait; the black dashed line represents the relationship between Ψ_{pd} and the response variable for the mean value of the trait; the black dotted line represents the relationship between Ψ_{pd} and the response variable for values corresponding to the mean -1 SD of the trait. Arrows indicate in each panel the direction of the trait effect. The scatterplots with the blue regression line indicate non-significant interactions. Each point represents a single measurement and each colour refers to a different species. Statistical significance of the interaction: * $p < 0.05$, ** $p < 0.01$, *** $p < 0.001$.

latter characterised by higher vulnerability to (drought) stress. In particular, higher SLA was associated with higher K_s and a less negative Ψ_{tlp} and Ψ_{50} , potentially linking physiological strategies with the plant economics spectrum theory, in line with previous studies (Zhu et al., 2018; Oliveira et al., 2021).

The second PCA axis (Fig. 2) accounts for the hydraulic sufficiency of leaves and allocation, as it is driven by K_t and H_v . This axis was less related than the first axis to the overall plant resistance to drought according to our a priori classification of species in drought resistance groups. For instance, while two of our most drought-resistant species (evergreen shrubs) do indeed present the highest values for PC₂ (*Quercus coccifera* and *Buxus sempervirens*) the other resistant species present values comparable to species more susceptible to drought.

4.2. Trait effects modulating drought responses

In this work we propose a novel conceptual framework to assess plant responses to drought that separates tissue-level drought exposure, physiological responses over time (relatively fast-changing) and the underlying (relatively slow-changing) functional traits (Kannenberg et al., 2022). Our results support the utility of this framework and show that functional traits modulate plant physiological responses and are therefore essential to understand and compare drought responses among

species (Volaire et al., 2020). Many previous studies have studied the regulation of leaf water potential (e.g., Martínez-Vilalta et al., 2014) and plant water use (e.g., Klein, 2014) as a function of exposure, characterised as the leaf predawn water potential (Ψ_{pd}). However, to the best of our knowledge, assessing the relationships between stomatal regulation, the plant water status and the modulating effect of the underlying traits (hydraulics, water relations, resource use) had never been assessed systematically, the only exceptions being the pioneering papers of Meinzer et al. (2016) and Fu and Meinzer (2019).

Our results suggest that species presenting a higher tolerance to drought (i.e., higher values of PC₁) have a looser regulation of the xylem water potentials and, correspondingly, a less strict stomatal control (Fig. 3). This finding can be interpreted through the notion that more resistant species can tolerate more negative water potentials, allowing them to have a less strict stomatal regulation of water loss, consistent with previous studies (Flo et al., 2021). A higher tolerance to drought would be therefore associated with a more “anisohydric” behaviour (Hochberg et al., 2018), in line with previous findings (Fu and Meinzer, 2019). This is also in accordance with the notion that xylem hydraulics limit drought tolerance (Brodribb and Cochard, 2009) and that stomatal sensitivity to leaf water potentials is strongly related to xylem characteristics (Klein, 2014). Interestingly, our data also shows that drought-tolerant species are able to regulate RWC more stringently with

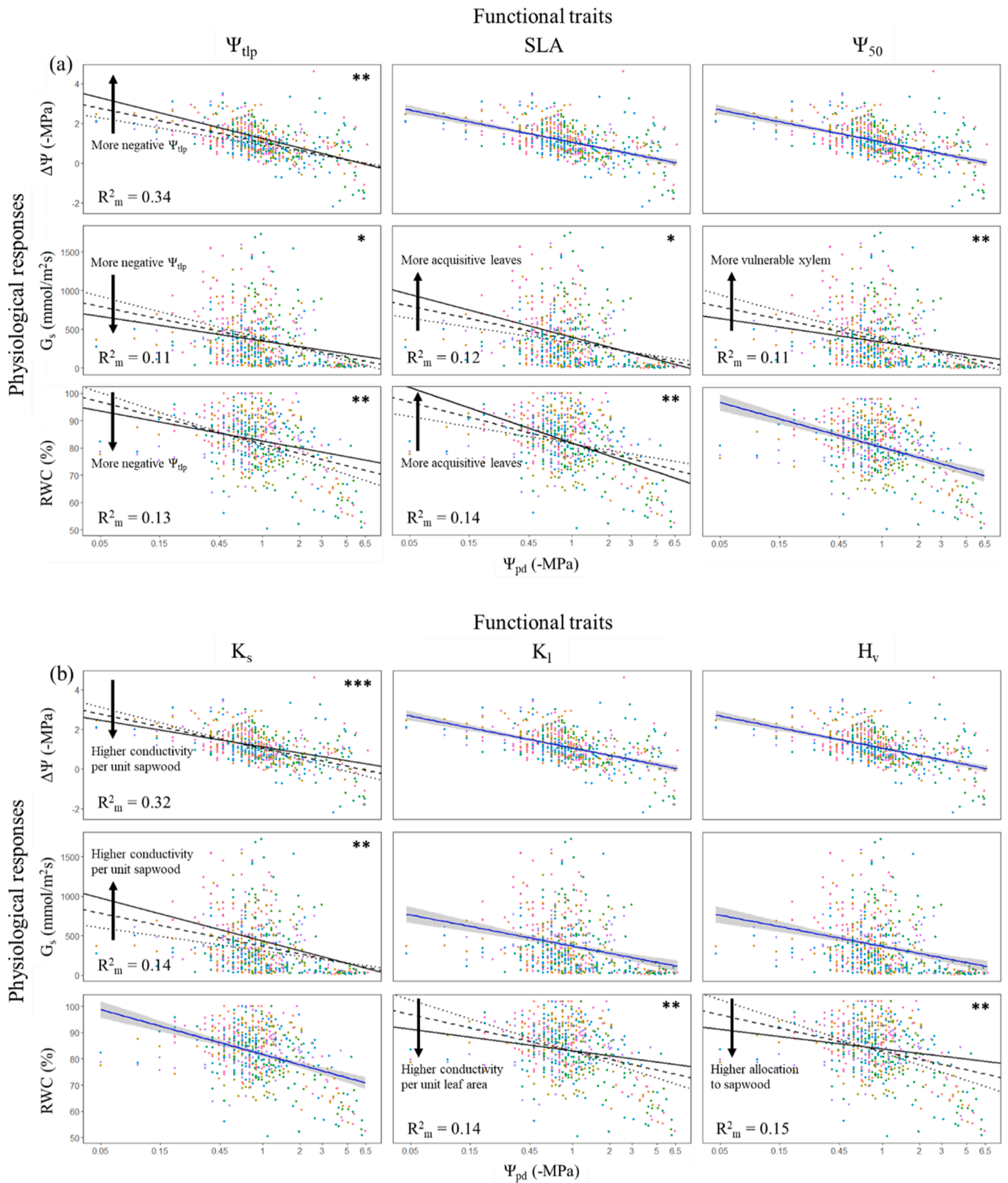


Fig. 4. Interaction plots of the relationship between physiological responses (G_s , $\Delta\Psi$, RWC) and tissue-level exposure to drought (Ψ_{pd}), modulated by individual functional traits. The black continuous line represents the relationship between Ψ_{pd} and the response variable for values corresponding to the mean plus one standard deviation (+1 SD) of the trait; the black dashed line represents the relationship between Ψ_{pd} and the response variable for the mean value of the trait; the black dotted line represents the relationship between Ψ_{pd} and the response variable for values corresponding to the mean -1 SD of the trait. Arrows indicate in each panel the direction of the trait effect. The scatterplots with the blue regression line indicate non-significant interactions. Each point represents a single measurement and each colour refers to a different species. Statistical significance of the interaction: * $p < 0.05$, ** $p < 0.01$, *** $p < 0.001$.

declining Ψ_{pd} (Fig. 3) compared to less drought tolerant species, thus showing an opposite pattern for the regulation of the water status in terms of RWC vs. its regulation in terms of leaf water potential. This result shows that drought-tolerant species may actually experience a lower risk of dehydration, despite their riskier (less stringent) behaviour in terms of leaf water potential and water use regulation. Although further studies are needed to assess the generality of this result, it may reflect wider safety margins in relatively anisohydric, embolism-resistant species (even if the leaf water potentials experienced may be much lower) (Garcia-Forner et al., 2016; Martin-StPaul et al., 2017) or higher capacity to retain water through higher solute concentrations in cells (more negative osmotic potential). The latter has already been reported for juniper relative to pines (Meinzer et al., 2014) or when comparing different grapevine cultivars (Hochberg et al., 2017; Sorek et al., 2021).

In addition, our results suggest that despite hydraulic sufficiency not explaining drought tolerance per se, it does contribute to defining the overall drought resistance strategies in our species. In fact, our results point to higher hydraulic sufficiency of leaves also being associated with a more effective regulation of RWC as Ψ_{pd} drops (Fig. 3). The enhanced ability to buffer RWC drops by higher drought tolerance and higher hydraulic sufficiency supports the notion that plants may show a diversity of strategies to achieve a relatively homeostatic regulation of RWC (Martinez-Vilalta et al., 2019; McDowell et al., 2022). The fact that water status regulation in terms of leaf water content vs. leaf water potential show opposite responses remains a novel and intriguing result that deserves further investigation.

4.3. The central role of Ψ_{tlp} in modulating physiological responses to drought

All our studied functional traits influenced, to some extent, the physiological responses to varying Ψ_{pd} . Nevertheless, Ψ_{tlp} stands out as it was the only functional trait modulating all our three response variables (Fig. 4a), thus playing an important role in defining the overall plant responses to drought, in line with previous studies (Blackman, 2018; Zhu et al., 2018). Ψ_{tlp} has long been considered a proxy of drought tolerance (Bartlett et al., 2012b; Blackman et al., 2010; Niinemets, 2001) as a more negative Ψ_{tlp} allows plants to maintain leaf turgor (Lenz et al., 2006) and stomatal opening (Mitchell et al., 2008) at more negative xylem water potentials, thus sustaining photosynthetic gas exchange and growth (Baltzer et al., 2008). A more negative Ψ_{tlp} is associated with a looser regulation of the $\Delta\Psi$ and a less stringent stomatal closing at increasingly higher levels of drought stress, thus relying on a more “anisohydric” strategy; which was ultimately better at buffering RWC during drought (Fig. 4a). Plants showing a less negative Ψ_{tlp} (i.e., drought “avoidant”) present a higher stomatal control and a tighter regulation of $\Delta\Psi$ as Ψ_{pd} drops, but our results indicate that these species’ ability to buffer the decrease in RWC under drought is limited.

An important caveat when comparing the relative importance of different traits in modulating physiological responses in our study is that vulnerability to embolism was obtained from the literature (species means) as opposed to the individual-level measurements conducted for all the other traits. Therefore, it remains possible that the higher importance of Ψ_{tlp} than Ψ_{50} in modulating physiological responses is explained by the higher level of detail in the former and hence remains to be confirmed by other studies. In addition, for K_s and K_l the fact that we measured relatively short segments implies that our estimates correspond mostly to lumen conductivity for the angiosperms and to total conductivity (lumen and wall) for the gymnosperms. Similarly, we assessed trait importance in determining responses to relatively mild drought and hence our results may not directly translate to more extreme conditions leading to drought-induced mortality.

5. Conclusion

This work aims at disentangling the complexity of plant responses to drought, accounting for (tissue-level) exposure and its interaction with functional traits to determine physiological responses in terms of the regulation of water status and use. We show that by explicitly differentiating between these variable types we can improve our understanding of plant responses to drought. Our study shows that species-level variability in functional traits can be summarised in two axes, one characterising increasing drought tolerance and decreasing acquisitiveness in resource use, and the other one characterising the hydraulic sufficiency of leaves and differences in resource allocation (i. e., wood vs leaves). Drought-tolerant species showed a less stringent regulation of water use and leaf water potential but were more effective at regulating leaf relative water content (RWC) within narrow limits. In addition, our results indicate that the leaf water potential at turgor loss point plays a central role in modulating all studied physiological responses to drought (stomatal regulation of water use and regulation of water status in terms of leaf water potential and RWC). The significant link between physiological responses and functional traits observed here paves the way for a trait-based understanding of the mechanisms underlying emergent drought resistance strategies in plants.

CRedit authorship contribution statement

JM-V, MM, EC and LS planned and designed the research; LS performed the measurements with contributions from PS-M, JM-V, MM, EC; LS analysed the data; and LS wrote the first draft with contributions from JM-V, EC, MM.

Declaration of Competing Interest

None declared.

Data Availability

Data will be made available on request.

Acknowledgements

We thank Lucía Galiano Pérez who curated the common garden experiment set up and who coordinated the experimental field campaigns. A special thanks go to Jiska Schaaf (MSc student), Irene Abad-Almendro, Ada Behncké-Serra, Álvaro Lázaro-Novell, Pol Magraso-Pérez, Laia Navarro-Irun, Pol Soler-Ruiz, Alba Teruel (BSc students) and Gemma Merino-Font (undergraduate student) whose contributions proved essentials for the development the research both as field and laboratory assistance. We also thank the researchers of the Forest Ecology Research Unit of CREAF for their valuable contributions to improve the scientific quality of the research. Finally, we want to thank Teresa Rosas for her valuable laboratory assistance. The research was supported by the Spanish Ministry of Economy and Competitiveness (MINECO) via competitive grant CGL2017-89149-C2-1-R (DRES-Sproject). LS was supported by an FPI scholarship from the MINECO, and his work was realised in the context of the doctoral program in Terrestrial ecology of the Autonomous University of Barcelona.

Appendix A. Supporting information

Supplementary data associated with this article can be found in the online version at [doi:10.1016/j.agwat.2023.108613](https://doi.org/10.1016/j.agwat.2023.108613).

References

- Allen, C.D., Breshears, D.D., McDowell, N.G., 2015. On underestimation of global vulnerability to tree mortality and forest die-off from hotter drought in the Anthropocene. *Ecosphere* 6, art129. <https://doi.org/10.1890/ES15-00203.1>.
- Anderegg, W.R.L., Wu, C., Acil, N., Carvalhais, N., Pugh, T.A.M., Sadler, J.P., Seidl, R., 2022. A climate risk analysis of Earth's forests in the 21st century. *Science* 377 (1979), 1099–1103. <https://doi.org/10.1126/science.abp9723>.
- Baltzer, J.L., Davies, S.J., Bunyavejchewin, S., Noor, N.S.M., 2008. The role of desiccation tolerance in determining tree species distributions along the Malay–Thai Peninsula. *Funct. Ecol.* 22, 221–231. <https://doi.org/10.1111/j.1365-2435.2007.01374.x>.
- Bartlett, M.K., Scoffoni, C., Ardy, R., Zhang, Y., Sun, S., Cao, K., Sack, L., 2012a. Rapid determination of comparative drought tolerance traits: using an osmometer to predict turgor loss point. *Methods Ecol. Evol.* 3 (5), 880–888. <https://doi.org/10.1111/j.2041-210X.2012.00230.x>.
- Bartlett, M.K., Scoffoni, C., Sack, L., 2012b. The determinants of leaf turgor loss point and prediction of drought tolerance of species and biomes: a global meta-analysis. *Ecol. Lett.* 15, 393–405. <https://doi.org/10.1111/j.1461-0248.2012.01751.x>.
- Bartlett, M.K., Klein, T., Jansen, S., Choat, B., Sack, L., 2016. The correlations and sequence of plant stomatal, hydraulic, and wilting responses to drought. *Proc. Natl. Acad. Sci.* 113, 13098–13103. <https://doi.org/10.1073/pnas.1604088113>.
- Blackman, C.J., 2018. Leaf turgor loss as a predictor of plant drought response strategies. *Tree Physiol.* 38, 655–657. <https://doi.org/10.1093/treephys/tpy047>.
- Blackman, C.J., Brodribb, T.J., Jordan, G.J., 2010. Leaf hydraulic vulnerability is related to conduit dimensions and drought resistance across a diverse range of woody angiosperms. *N. Phytol.* 188, 1113–1123. <https://doi.org/10.1111/j.1469-8137.2010.03439.x>.
- Brodribb, T.J., Cochard, H., 2009. Hydraulic failure defines the recovery and point of death in water-stressed conifers. *Plant Physiol.* 149, 575–584. <https://doi.org/10.1104/pp.108.129783>.
- Brodribb, T.J., Powers, J., Cochard, H., Choat, B., 2020. Hanging by a thread? Forests and drought. *Science* 368 (1979), 261–266. <https://doi.org/10.1126/science.aat7631>.
- Choat, B., Brodribb, T.J., Brodersen, C.R., Duursma, R.A., López, R., Medlyn, B.E., 2018. Triggers of tree mortality under drought. *Nature* 558, 531–539. <https://doi.org/10.1038/s41586-018-0240-x>.
- Cochard, H., Peiffer, M., le Gall, K., Andre, G., 1997. Developmental control of xylem hydraulic resistances and vulnerability to embolism in *Fraxinus excelsior* L.: impacts on water relations. *J. Exp. Bot.* 48, 655–663. <https://doi.org/10.1093/jxb/48.3.655>.
- Cochard, H., Damour, G., Bodet, C., Tharwat, I., Poirier, M., Améglio, T., 2005. Evaluation of a new centrifuge technique for rapid generation of xylem vulnerability curves. *Physiol. Plant* 124, 410–418. <https://doi.org/10.1111/j.1399-3054.2005.00526.x>.
- Duursma, R.A., Blackman, C.J., López, R., Martin-StPaul, N.K., Cochard, H., Medlyn, B.E., 2019. On the minimum leaf conductance: its role in models of plant water use, and ecological and environmental controls. *N. Phytol.* 221, 693–705. <https://doi.org/10.1111/nph.15395>.
- Fernández-García, N., Olmos, E., Bardisi, E., García-De la Garma, J., López-Berenguer, C., Rubio-Asensio, J.S., 2014. Intrinsic water use efficiency controls the adaptation to high salinity in a semi-arid adapted plant, henna (*Lawsonia inermis* L.). *J. Plant Physiol.* 171, 64–75. <https://doi.org/10.1016/j.jplph.2013.11.004>.
- Flo, V., Martínez-Vilalta, J., Mencuccini, M., Granda, V., Anderegg, W.R.L., Poyatos, R., 2021. Climate and functional traits jointly mediate tree water-use strategies. *N. Phytol.* 231, 617–630. <https://doi.org/10.1111/nph.17404>.
- Fu, X., Meinzer, F.C., 2019. Metrics and proxies for stringency of regulation of plant water status (iso/anisohydry): a global data set reveals coordination and trade-offs among water transport traits. *Tree Physiol.* 39, 122–134. <https://doi.org/10.1093/treephys/tpy087>.
- García-Fórner, N., Adams, H.D., Sevanto, S., Collins, A.D., Dickman, L.T., Hudson, P.J., Zeppel, M.J.B., Jenkins, M.W., Powers, H., Martínez-Vilalta, J., McDowell, N.G., 2016. Responses of two semiarid conifer tree species to reduced precipitation and warming reveal new perspectives for stomatal regulation. *Plant Cell Environ.* 39, 38–49. <https://doi.org/10.1111/pce.12588>.
- García-Valdés, R., Vayreda, J., Retana, J., Martínez-Vilalta, J., 2021. Low forest productivity associated with increasing drought-tolerant species is compensated by an increase in drought-tolerance richness. *Glob. Change Biol.* 27, 2113–2127. <https://doi.org/10.1111/gcb.15529>.
- Gleason, S.M., Westoby, M., Jansen, S., Choat, B., Hacke, U.G., Pratt, R.B., Bhaskar, R., Brodribb, T.J., Bucci, S.J., Cao, K., Cochard, H., Delzon, S., Domec, J., Fan, Z., Feild, T.S., Jacobsen, A.L., Johnson, D.M., Lens, F., Maherali, H., Martínez-Vilalta, J., Mayr, S., McCulloh, K.A., Mencuccini, M., Mitchell, P.J., Morris, H., Nardini, A., Pittermann, J., Plavcová, L., Schreiber, S.G., Sperry, J.S., Wright, L.J., Zanne, A.E., 2016. Weak tradeoff between xylem safety and xylem-specific hydraulic efficiency across the world's woody plant species. *N. Phytol.* 209, 123–136. <https://doi.org/10.1111/nph.13646>.
- Hochberg, U., Bonel, A.G., David-Schwartz, R., Degu, A., Fait, A., Cochard, H., Peterlunger, E., Herrera, J.C., 2017. Grapevine acclimation to water deficit: the adjustment of stomatal and hydraulic conductance differs from petiole embolism vulnerability. *Planta* 245, 1091–1104. <https://doi.org/10.1007/s00425-017-2662-3>.
- Hochberg, U., Rockwell, F.E., Holbrook, N.M., Cochard, H., 2018. Iso/Anisohydry: a plant–environment interaction rather than a simple hydraulic trait. *Trends Plant Sci.* 23, 112–120. <https://doi.org/10.1016/j.tplants.2017.11.002>.
- Huang, C., Becker, M.F., Keto, J.W., Kovar, D., 2007. Annealing of nanostructured silver films produced by supersonic deposition of nanoparticles. *J. Appl. Phys.* 102, 054308. <https://doi.org/10.1063/1.2776163>.
- Kannenberg, S.A., Guo, J.S., Novick, K.A., Anderegg, W.R.L., Feng, X., Kennedy, D., Konings, A.G., Martínez-Vilalta, J., Matheny, A.M., 2022. Opportunities, challenges and pitfalls in characterizing plant water-use strategies. *Funct. Ecol.* 36, 24–37. <https://doi.org/10.1111/1365-2435.13945>.
- Klein, T., 2014. The variability of stomatal sensitivity to leaf water potential across tree species indicates a continuum between isohydric and anisohydric behaviours. *Funct. Ecol.* 28, 1313–1320. <https://doi.org/10.1111/1365-2435.12289>.
- Lecina-Díaz, J., Martínez-Vilalta, J., Alvarez, A., Banqué, M., Birkmann, J., Feldmeyer, D., Vayreda, J., Retana, J., 2021. Characterizing forest vulnerability and risk to climate-change hazards. *Front. Ecol. Environ.* 19, 126–133. <https://doi.org/10.1002/fee.2278>.
- Lenz, T.I., Wright, I.J., Westoby, M., 2006. Interrelations among pressure-volume curve traits across species and water availability gradients. *Physiol. Plant* 127, 423–433. <https://doi.org/10.1111/j.1399-3054.2006.00680.x>.
- Levitt, J., 1980. Responses of plants to environmental stresses. Volume II: Water, Radiation, Salt, and other Stresses. Academic Press, New York.
- Liu, H., Ye, Q., Gleason, S.M., He, P., Yin, D., 2021. Weak tradeoff between xylem hydraulic efficiency and safety: climatic seasonality matters. *N. Phytol.* 229, 1440–1452. <https://doi.org/10.1111/nph.16940>.
- Marksteijn, L., Poorter, L., Bongers, F., Paz, H., Sack, L., 2011. Hydraulics and life history of tropical dry forest tree species: coordination of species' drought and shade tolerance. *N. Phytol.* 191, 480–495. <https://doi.org/10.1111/j.1469-8137.2011.03708.x>.
- Martínez-Vilalta, J., Anderegg, W.R.L., Sapes, G., Sala, A., 2019. Greater focus on water pools may improve our ability to understand and anticipate drought-induced mortality in plants. *N. Phytol.* 223, 22–32. <https://doi.org/10.1111/nph.15644>.
- Martínez-Vilalta, J., García-Fórner, N., 2017. Water potential regulation, stomatal behaviour and hydraulic transport under drought: deconstructing the iso/anisohydric concept. *Plant Cell Environ.* 40, 962–976. <https://doi.org/10.1111/pce.12846>.
- Martínez-Vilalta, J., Mencuccini, M., Vayreda, J., Retana, J., 2010. Interspecific variation in functional traits, not climatic differences among species ranges, determines demographic rates across 44 temperate and Mediterranean tree species. *J. Ecol.* 98, 1462–1475. <https://doi.org/10.1111/j.1365-2745.2010.01718.x>.
- Martínez-Vilalta, J., Poyatos, R., Aguadé, D., Retana, J., Mencuccini, M., 2014. A new look at water transport regulation in plants. *N. Phytol.* 204, 105–115. <https://doi.org/10.1111/nph.12912>.
- Martin-StPaul, N., Delzon, S., Cochard, H., 2017. Plant resistance to drought depends on timely stomatal closure. *Ecol. Lett.* 20, 1437–1447. <https://doi.org/10.1111/ele.12851>.
- McDowell, N.G., Allen, C.D., Anderson-Teixeira, K., Aukema, B.H., Bond-Lamberty, B., Chini, L., Clark, J.S., Dietze, M., Grossiord, C., Hanbury-Brown, A., Hurtt, G.C., Jackson, R.B., Johnson, D.J., Kueppers, L., Lichstein, J.W., Ogle, K., Poulter, B., Pugh, T.A.M., Seidl, R., Turner, M.G., Uriarte, M., Walker, A.P., Xu, C., 2020. Pervasive shifts in forest dynamics in a changing world. *Science* 368 (1979). <https://doi.org/10.1126/science.aaz9463>.
- McDowell, N.G., Sapes, G., Pivovarov, A., Adams, H.D., Allen, C.D., Anderegg, W.R.L., Arend, M., Breshears, D.D., Brodribb, T., Choat, B., Cochard, H., de Cáceres, M., de Kauwe, M.G., Grossiord, C., Hammond, W.M., Hartmann, H., Hoch, G., Kahmen, A., Klein, T., Mackay, D.S., Mantova, M., Martínez-Vilalta, J., Medlyn, B.E., Mencuccini, M., Nardini, A., Oliveira, R.S., Sala, A., Tissue, D.T., Torres-Ruiz, J.M., Trowbridge, A.M., Trugman, A.T., Wiley, E., Xu, C., 2022. Mechanisms of woody-plant mortality under rising drought, CO₂ and vapour pressure deficit. *Nat. Rev. Earth Environ.* 3, 294–308. <https://doi.org/10.1038/s43017-022-00272-1>.
- Meinzer, F.C., Woodruff, D.R., Marias, D.E., McCulloh, K.A., Sevanto, S., 2014. Dynamics of leaf water relations components in co-occurring iso- and anisohydric conifer species. *Plant Cell Environ.* 37, 2577–2586. <https://doi.org/10.1111/pce.12327>.
- Meinzer, F.C., Woodruff, D.R., Marias, D.E., Smith, D.D., McCulloh, K.A., Howard, A.R., Magedman, A.L., 2016. Mapping 'hydroscales' along the iso- to anisohydric continuum of stomatal regulation of plant water status. *Ecol. Lett.* 19, 1343–1352. <https://doi.org/10.1111/ele.12670>.
- Mitchell, P.J., Veneklaas, E.J., Lambers, H., Burgess, S.S.O., 2008. Leaf water relations during summer water deficit: differential responses in turgor maintenance and variation in leaf structure among different plant communities in south-western Australia. *Plant Cell Environ.* 31, 1791–1802. <https://doi.org/10.1111/j.1365-3040.2008.01882.x>.
- Niinemets, Ü., 2001. Global-scale climatic controls of leaf dry mass per area, density, and thickness in trees and shrubs. *Ecology* 82, 453–469. [https://doi.org/10.1890/0012-9658\(2001\)082\[0453:GSCCOL\]2.0.CO;2](https://doi.org/10.1890/0012-9658(2001)082[0453:GSCCOL]2.0.CO;2).
- Niinemets, Ü., Valladares, F., 2006. Tolerance to shade, drought, and waterlogging of temperate northern hemisphere trees and shrubs. *Ecol. Monogr.* 76, 521–547. [https://doi.org/10.1890/0012-9615\(2006\)076\[0521:TSDAW\]2.0.CO;2](https://doi.org/10.1890/0012-9615(2006)076[0521:TSDAW]2.0.CO;2).
- Ogaya, R., Peñuelas, J., Martínez-Vilalta, J., Mangirón, M., 2003. Effect of drought on diameter increment of *Quercus ilex*, *Phillyrea latifolia*, and *Arbutus unedo* in a holm oak forest of NE Spain. *Ecol. Manag.* 180, 175–184. [https://doi.org/10.1016/S0378-1127\(02\)00598-4](https://doi.org/10.1016/S0378-1127(02)00598-4).
- Oliveira, R.S., Eller, C.B., Barros, F. de v., Hirota, M., Brum, M., Bittencourt, P., 2021. Linking plant hydraulics and the fast-slow continuum to understand resilience to drought in tropical ecosystems. *N. Phytol.* 230, 904–923. <https://doi.org/10.1111/nph.17266>.
- R Core Team, 2019. R: A language and environment for statistical computing. R Foundation for Statistical Computing, Vienna, Austria. (<https://www.R-project.org/>).
- Reich, P.B., 2014. The world-wide 'fast-slow' plant economics spectrum: a traits manifesto. *J. Ecol.* 102, 275–301. <https://doi.org/10.1111/1365-2745.12211>.

- Rosas, T., Mencuccini, M., Barba, J., Cochard, H., Saura-Mas, S., Martínez-Vilalta, J., 2019. Adjustments and coordination of hydraulic, leaf and stem traits along a water availability gradient. *N. Phytol.* 223, 632–646. <https://doi.org/10.1111/nph.15684>.
- Rosas, T., Mencuccini, M., Batlles, C., Regalado, Í., Saura-Mas, S., Sterck, F., Martínez-Vilalta, J., 2021. Are leaf, stem and hydraulic traits good predictors of individual tree growth? *Funct. Ecol.* 35, 2435–2447. <https://doi.org/10.1111/1365-2435.13906>.
- Sanchez-Martinez, P., Martínez-Vilalta, J., Dexter, K.G., Segovia, R.A., Mencuccini, M., 2020. Adaptation and coordinated evolution of plant hydraulic traits. *Ecol. Lett.* 23, 1599–1610. <https://doi.org/10.1111/ele.13584>.
- Savi, T., Tintner, J., da Sois, L., Grabner, M., Petit, G., Rosner, S., 2019. The potential of mid-infrared spectroscopy for prediction of wood density and vulnerability to embolism in woody angiosperms. *Tree Physiol.* 39, 503–510. <https://doi.org/10.1093/treephys/tpy112>.
- Seidl, R., Thom, D., Kautz, M., Martin-Benito, D., Peltoniemi, M., Vacchiano, G., Wild, J., Ascoli, D., Petr, M., Honkaniemi, J., Lexer, M.J., Trotsiuk, V., Mairota, P., Svoboda, M., Fabrika, M., Nagel, T.A., Reyer, C.P.O., 2017. Forest disturbances under climate change. *Nat. Clim. Change* 7, 395–402. <https://doi.org/10.1038/nclimate3303>.
- Sorek, Y., Greenstein, S., Netzer, Y., Shtein, I., Jansen, S., Hochberg, U., 2021. An increase in xylem embolism resistance of grapevine leaves during the growing season is coordinated with stomatal regulation, turgor loss point and intervessel pit membranes. *N. Phytol.* 229, 1955–1969. <https://doi.org/10.1111/nph.17025>.
- Vilà-Cabrera, A., Martínez-Vilalta, J., Retana, J., 2015. Functional trait variation along environmental gradients in temperate and Mediterranean trees. *Glob. Ecol. Biogeogr.* 24, 1377–1389.
- Villanueva, J.A. (ed.). (2005). Tercer Inventario Forestal Nacional (1997–2007). Ed. Ministerio de Medio Ambiente. Madrid. (<https://www.miteco.gob.es/es/biodiversidad/servicios/banco-datos-naturaleza/informacion-disponible/ifn3.html>).
- Voltaire, F., Gleason, S.M., Delzon, S., 2020. What do you mean “functional” in ecology? Patterns versus processes. *Ecol. Evol.* 10, 11875–11885. <https://doi.org/10.1002/ece3.6781>.
- Wheeler, J.K., Huggett, B.A., Tofte, A.N., Rockwell, F.E., Holbrook, N.M., 2013. Cutting xylem under tension or supersaturated with gas can generate PLC and the appearance of rapid recovery from embolism (n/a-n/a). *Plant Cell Environ.* 36. <https://doi.org/10.1111/pce.12139>.
- Wright, I.J., Reich, P.B., Westoby, M., Ackerly, D.D., Baruch, Z., Bongers, F., Cavender-Bares, J., Chapin, T., Cornelissen, J.H.C., Diemer, M., Flexas, J., Garnier, E., Groom, P.K., Gulias, J., Hikosaka, K., Lamont, B.B., Lee, T., Lee, W., Lusk, C., Midgley, J.J., Navas, M.-L., Niinemets, Ü., Oleksyn, J., Osada, N., Poorter, H., Poot, P., Prior, L., Pyankov, V.I., Roumet, C., Thomas, S.C., Tjoelker, M.G., Veneklaas, E.J., Villar, R., 2004. The worldwide leaf economics spectrum. *Nature* 428, 821–827. <https://doi.org/10.1038/nature02403>.
- Zhu, S.D., Chen, Y.J., Ye, Q., He, P.C., Liu, H., Li, R.H., Fu, P.L., Jiang, G.F., Cao, K.F., 2018. Leaf turgor loss point is correlated with drought tolerance and leaf carbon economics traits. *Tree Physiol.* 38, 658–663. <https://doi.org/10.1093/treephys/tpy013>.